Organic Chemistry Frontiers c6qo00760k

1

Rhodanine-based dyes absorbing in the entire visible spectrum

Rafael Sandoval-Torrientes, Joaquín Calbo, David García-Fresnadillo, José Santos, Enrique Ortí* and Nazario Martín*

A series of new broad-absorbing dyes based on rhodanine derivatives conjugated with triarylamines through a fluorene backbone were synthesized. Spectroscopic and electrochemical characterizations, along with theoretical calculations, revealed interesting properties of the dyes that efficiently absorb in the entire visible spectrum.

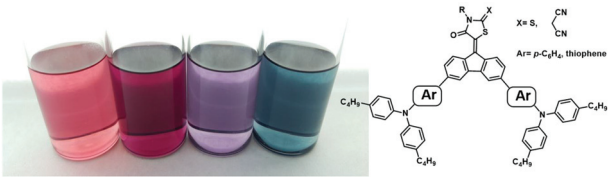

Q4

Please check this proof carefully. **Our staff will not read it in detail after you have returned it.**

Translation errors between word-processor files and typesetting systems can occur so the whole proof needs to be read. Please pay particular attention to: tabulated material; equations; numerical data; figures and graphics; and references. If you have not already indicated the corresponding author(s) please mark their name(s) with an asterisk. Please e-mail a list of corrections or the PDF with electronic notes attached – do not change the text within the PDF file or send a revised manuscript. Corrections at this stage should be minor and not involve extensive changes. All corrections must be sent at the same time.

Please bear in mind that minor layout improvements, e.g. in line breaking, table widths and graphic placement, are routinely applied to the final version.

We will publish articles on the web as soon as possible after receiving your corrections; **no late corrections will be made**.

Please return your **final** corrections, where possible within **48 hours** of receipt, by e-mail to: OrgChemFrontiersPROD@rsc.org

Queries for the attention of the authors

Journal: **Organic Chemistry Frontiers**

Paper: **c6qo00760k**

Title: **Rhodanine-based dyes absorbing in the entire visible spectrum**

Editor's queries are marked like this [Q1, Q2, ...], and for your convenience line numbers are indicated like this [5, 10, 15, ...].

Please ensure that all queries are answered when returning your proof corrections so that publication of your article is not delayed.

Query Reference	Query	Remarks
Q1	For your information: You can cite this article before you receive notification of the page numbers by using the following format: (authors), Org. Chem. Front., (year), DOI: 10.1039/c6qo00760k.	
Q2	Please carefully check the spelling of all author names. This is important for the correct indexing and future citation of your article. No late corrections can be made.	
Q3	Do you wish to add an e-mail address for the corresponding author? If so, please supply the e-mail address.	
Q4	Please check that the Graphical Abstract text fits within the allocated space indicated on the front page of the proof. If the entry does not fit between the two horizontal lines, then please trim the text and/or the title.	
Q5	The sentence beginning "Spectroscopic and..." has been altered for clarity, please check that the meaning is correct.	
Q6	The sentence beginning "However, in..." has been altered for clarity, please check that the meaning is correct.	
Q7	The sentence beginning "Once the ability of..." has been altered for clarity, please check that the meaning is correct.	
Q8	The sentence beginning "By employing both..." has been altered for clarity, please check that the meaning is correct.	
Q9	The sentence beginning "To date, in all the previously..." has been altered for clarity, please check that the meaning is correct.	
Q10	The sentence beginning "All Knoevenagel reactions..." has been altered for clarity, please check that the meaning is correct.	
Q11	The sentence beginning "Moreover, the..." has been altered for clarity, please check that the meaning is correct.	
Q12	"Wavelength" appears to be spelled incorrectly in Fig. 1 (b). Please could you supply a corrected version (preferably as a TIF file at 600 dots per inch) with your proof corrections.	

Q13	The sentence beginning “Minimum-energy…” has been altered for clarity, please check that the meaning is correct.	
Q14	The sentence beginning “Moving to higher…” has been altered for clarity, please check that the meaning is correct.	

ORGANIC CHEMISTRY FRONTIERS

RESEARCH ARTICLE

Rhodanine-based dyes absorbing in the entire visible spectrum†

Cite this: DOI: 10.1039/c6qo00760k

Rafael Sandoval-Torrientes,[a] Joaquín Calbo,[b] David García-Fresnadillo,[c] José Santos,[a] Enrique Ortí*[b] and Nazario Martín*[a,c]

Received 28th November 2016,
Accepted 3rd February 2017
DOI: 10.1039/c6qo00760k
rsc.li/frontiers-organic

A series of new broad-absorbing dyes based on rhodanine derivatives conjugated with triarylamines using a fluorene backbone was synthesized. Spectroscopic and electrochemical characterizations, along with theoretical calculations at the B3LYP/cc-pVDZ level, revealed interesting properties of the dyes, which make the dyes efficiently absorb in the entire visible spectrum.

Since environmental problems derived from the overconsumption of fossil fuels have started to manifest, many resources have been allocated in search of new environmentally friendly energy sources. Among these sources, solar energy probably represents the most abundant and available source of energy. Over the last 15 years, organic photovoltaics have experienced slow but sustained progress.[1] From the earliest poly(*p*-phenylene vinylene) devices (with the low 3% power conversion efficiency (PCE))[2–4] to the poly(3-hexylthiophene-2,5-diyl) devices (with 5% PCE)[5–7] and the state-of-the-art donor–acceptor (D–A) photovoltaic devices (with 11% PCE),[8–12] the most common feature of these materials is their polymeric nature. However, in the last few years, more and more systems based on small molecules have been developed with efficiencies comparable to those of their polymer counterparts.[13–15] Once the ability of small molecules to efficiently perform like polymers was demonstrated, the race to develop new dyes that are able to broadly harvest light in the visible-near infrared region (where most of the solar spectrum is centred) started.

Several groups have recently incorporated the electron-deficient, rhodanine end-capping group to a series of electron-rich systems, allowing the fabrication of devices with efficiencies ranging from 5 to 9%.[13,15,16–18] All these systems share A–D–A structures in common, with rhodanines linked to the central core by a Knoevenagel condensation reaction with an aldehyde group. Herein, we report for the first time four new molecules (**RFTA-1–4**, see Scheme 1) *via* incorporating rhodanine (R) derivatives into a fluorene (F) backbone (through its C9 position), giving rise to D–A–D structures (employing triarylamine (TA) as electron-donating groups) that feature absorption spectra spanning the entire visible region. Spectroscopic and electrochemical studies, complemented by density functional theory (DFT) calculations, provide clear insight into the electronic and optical properties of these novel dyes.

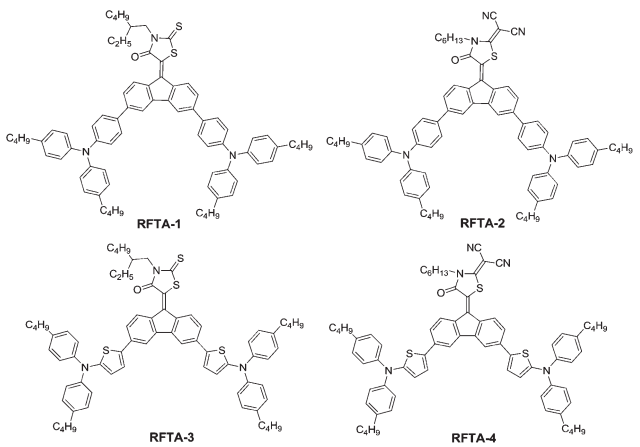

Scheme 1 Rhodanine/fluorene/triarylamine (RFTA) dyes.

All the synthesized dyes share a central fluorene core bearing either *N*-hexyl-2-(1,1-dicyanomethylene)rhodanine or *N*-(2-ethylhexylrhodanine) on its C9 position and two triarylamines (triphenylamine or diphenylaminothiophene) on positions C3 and C6. By employing both electron donors and acceptors of different relative strengths, we were able to fine-tune the light absorption properties of the dyes, which made the dyes cover the whole visible spectral range with different λ_{max}. From the synthetic point of view, the most remarkable achievement was the insertion, for the first time (to the best of our knowledge), of a rhodanine fragment into the C9 position of the fluorene core. This opened the door to the use of

[a]*IMDEA-Nanociencia, Ciudad Universitaria de Cantoblanco, 28049 Madrid, Spain*
[b]*Instituto de Ciencia Molecular, Universidad de Valencia, 46980 Paterna, Spain*
[c]*Departamento de Química Orgánica, Facultad de Ciencias Químicas, Universidad Complutense de Madrid, 28040 Madrid, Spain*

†Electronic supplementary information (ESI) available: Experimental details, synthesis, structural and photophysical characterization, cyclic voltammograms, NMR spectra, and theoretical calculations. See DOI: 10.1039/c6qo00760k

rhodanine acceptors as central units in D–A–D type structures, thus complementing their former use as terminal moieties in A–D–A-type systems. Another interesting aspect is the gain in the planarity and rigidity of the rhodanine/fluorene accepting core. To date, in all the previously described dyes containing the rhodanine fragments, the fragments were attached *via* a Knoevenagel condensation with an aldehyde group on the side of the main molecular skeleton, thus resulting in molecules lacking the rigidity that we herein were able to provide.

As depicted in Scheme 2, triarylamine products were obtained by a Suzuki cross-coupling reaction of 3,6-dibromofluorenone (**1**)[19] with boronic ester **2**,[20] followed by a Knoevenagel condensation of the resulting product **3** with either rhodanine **6** or **7** to obtain the products **RFTA-1** and **RFTA-2**, respectively. In the case of the diarylaminothiophene systems, its corresponding organotin derivative **10** was prepared as depicted in Scheme S2† in the ESI,† and then coupled by a Stille cross-coupling reaction with **1**. Further Knoevenagel condensation with the corresponding rhodanine provided products **RFTA-3** and **RFTA-4**. All Knoevenagel reactions provided products in moderate to low yields. Moreover, the unreacted starting materials were easily recovered and were repeatedly used again until their full conversion. Full synthetic details are available in the ESI.†

All RFTA dyes showed strong absorption in the visible region of the spectrum (Table 1 & Fig. S2, S3 in the ESI†), featuring a single broad band that red-shifted and broadened as stronger acceptors and/or donors were attached to the fluorene core (see Fig. 1a). The first compound of the series (**RFTA-1**), bearing rhodanine as an acceptor and triphenylamine (TPA) as a donor, exhibited peaks at 523 nm with its onset at 653 nm. When the stronger electron-accepting 2-(1,1-dicyanomethylene)rhodanine **7** was introduced (**RFTA-2**), the molecular absorption caused a 20 nm red shift, peaking at 545 nm with an onset at 692 nm. A more dramatic bathochromic effect was observed with rhodanine as an acceptor and diphenylaminothiophene (DPAT) as a donor (**RFTA-3**). In this case, the absorption was centered at 565 nm, representing a 40 nm shift, with an onset at 748 nm. Finally, **RFTA-4** had the strongest donor and acceptor moieties and showed a broad absorption band centered at 590 nm with the onset at 786 nm. The bathochromic shift observed in λ_{abs}^{max} on increasing the donor and acceptor strengths of the substituent groups suggests that this band, showing quite large molar absorption coefficients (1.6–2.3 × 10^4 M^{-1} cm^{-1}), may be attributed to an intramolecular charge transfer (ICT) process, according to previously described fluorenone derivatives bearing electron-donating groups.[21] Solvatochromic experiments demonstrated noticeable shifts in the lower energy absorption peak (Fig. S2, in the ESI†), thus providing extra evidence of its suggested ICT nature. In addition, the significant broadening of this

Table 1 Photophysical properties of **RFTA-1–4** dyes and their **3** & **5** precursors measured in CH_2Cl_2 solution

Dye	λ_{abs}^{max} [nm]	λ_{onset} [a] [nm]	$\varepsilon \times 10^4$ [M^{-1} cm^{-1}]	λ_{em}^{max} [nm]	E_{0-0} [b] [eV]	Φ_{em} [c]
RFTA-1	523	653	1.64	1019	1.79	0.008
RFTA-2	545	692	2.34	1043	1.73	0.006
RFTA-3	565	748	1.93	1013	1.71	0.011
RFTA-4	590	786	2.34	1036	1.65	0.010
3	440	—	—	707	2.29	0.027
5	483	—	—	709	2.16	0.030

[a] Estimated extrapolation from the absorption feature edge to $A = 0$. [b] Uncertainty ±5%. [c] Uncertainty ±20%.

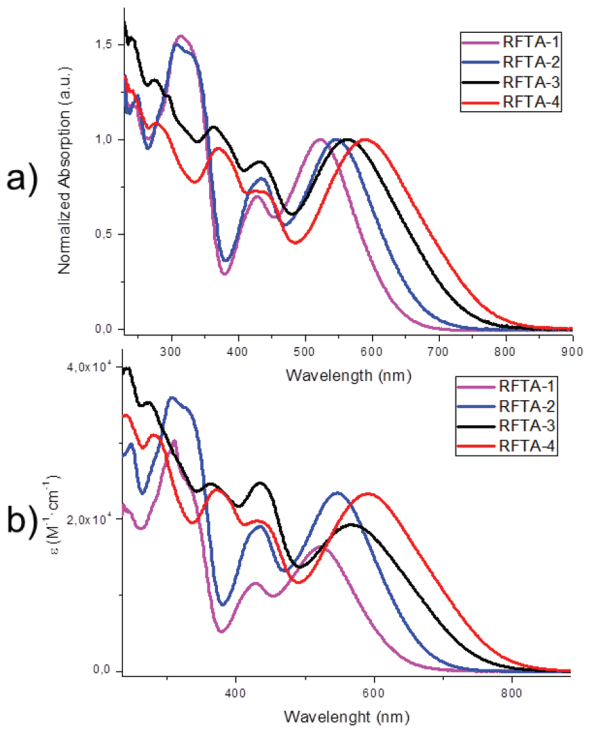

Fig. 1 (a) Normalized UV-vis absorption spectra of RFTA dyes in CH_2Cl_2 solution. (b) Molar absorption profiles.

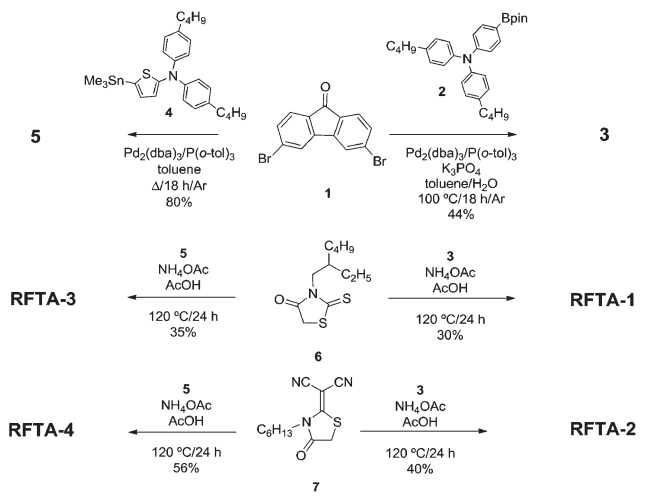

Scheme 2 Synthetic route to rhodanine-based compounds **RFTA-1–4**.

absorption band for compounds **RFTA-3** and **RFTA-4** is noteworthy. As has been discussed below, based on theoretical calculations, this effect was attributed to larger conjugation between the DPAT units and the fluorene core provided by the thiophene rings.

Regarding the emission features of **RFTA** compounds (Table 1, Fig. S4–S6,† in the ESI†), their emission maxima (λ_{em}^{max}) are strongly red-shifted (Stokes' shifts of *ca.* 9000 cm^{-1} for **RFTA-1** and **RFTA-2** (*ca.* 500 nm) and *ca.* 7500 cm^{-1} for **RFTA-3** and **RFTA-4** (*ca.* 450 nm)) with respect to that of their precursors **3** and **5** (Stokes' shifts of 8600 cm^{-1} (267 nm) and 6600 cm^{-1} (226 nm), respectively; *cf.* 6800 cm^{-1} (130 nm) for 9*H*-fluoren-9-one[21d] in polar aprotic solvent). This again demonstrates the important role played by the structural features since **RFTA-2** and **RFTA-4**, bearing (dicyanomethylene) rhodanine moieties, have larger λ_{em}^{max} values. Additionally, the combination of lower LUMO energies for **RFTA-2** and **RFTA-4** and higher HOMO energies for **RFTA-3** and **RFTA-4** (including the DPAT feature) explains the lower energy values for the 0–0 transition (E_{0-0}, Table 1) for **RFTA-3** and **RFTA-4**. This is in excellent agreement with the results obtained from electrochemistry and theoretical calculations, *vide infra*. On the other hand, the low-emission quantum yields determined for all the **RFTA** compounds (1% or below) reflect the fact that excited state deactivation by fluorescence is of little importance compared to that by non-radiative processes. This agrees with the energy gap law stating that the lower the gap between the ground and excited state, the less efficient the radiative processes.

The electrochemical properties of the new RFTA dyes were studied by cyclic voltammetry (CV). All molecules showed an amphoteric redox behavior, presenting one oxidation and two reduction processes (see Table 2 and Fig. S1, in the ESI†). For **RFTA-1** and **RFTA-2**, both bearing the TPA donor, the oxidation potentials were identical (1.05 V). However, a significant 100 mV anodic shift was observed for the first reduction potential while moving from **RFTA-1** (−0.61 V) to **RFTA-2** (−0.51 V), bearing a stronger electron-accepting rhodanine group. Similarly, the second reduction potential experienced a moderate 50 mV anodic shift.

Table 2 Electrochemical data for the ground and excited states of dyes **RFTA-1–4**

Dye	$E_{1/2}^{ox}$ [a] [V]	$E_{1/2}^{red1}$ [a] [V]	E_{gap}^{cv} [b] [V]	E_{HOMO}/E_{LUMO} [c] [eV]	E^{ox*} [d] [V]	E^{red*} [d] [V]
RFTA-1	1.05	−0.61	1.66	−5.45/−3.79	−0.74	1.18
RFTA-2	1.05	−0.51	1.56	−5.45/−3.89	−0.68	1.22
RFTA-3	0.92	−0.61	1.53	−5.32/−3.79	−0.74	1.10
RFTA-4	0.94	−0.48	1.42	−5.34/−3.92	−0.71	1.19

[a] Measured by CV in CH_2Cl_2 solution using 0.1 M Bu_4NPF_6 as the supporting electrolyte, glassy carbon as the working electrode, and Pt wires as the reference and counter electrodes; all potentials were obtained *vs.* Fc/Fc^+ as an internal reference. [b] Electrochemical gap determined as E_{ox}–E_{red}. [c] HOMO/LUMO energies estimated according to $E_{HOMO} = -[E_{1/2}^{ox} + 4.4]$ eV; $E_{LUMO} = E_{HOMO} + E_{gap}^{cv}$. [d] Excited state redox potentials, uncertainty 5%.

When the stronger DPAT donor was used (**RFTA-3** and **RFTA-4**), the oxidation potential experienced a 130 and 110 mV cathodic shift, respectively. In the case of **RFTA-3**, with the same rhodanine acceptor as **RFTA-1**, there was no change for the first reduction potential (−0.61 V). However, **RFTA-4**, bearing the strongest acceptor, showed a 30 mV anodic shift compared to **RFTA-2** and presented the smallest reduction potential (−0.48 V). This difference was ascribed to experimental error. The calculated electrochemical gaps ranged from 1.66 to 1.44 eV, diminishing from **RFTA-1** to **RFTA-4**, which is in good agreement with the trend inferred from the spectroscopic data (Table 1).

Concerning the redox potentials of the excited states (Table 2), while the oxidation process from RFTA* to $RFTA^+$ had similar potentials for all the RFTA dyes, the reduction process from RFTA* to $RFTA^-$ seems to be slightly less favored in the case of **RFTA-3**, lacking the TPA (less coplanar/less electronically coupled donor, *vide infra*) and dicyanomethylene (stronger acceptor) moieties.

To gain insight into the optical and electronic properties of the novel rhodanine-based dyes, theoretical calculations were performed within the density functional theory (DFT) framework (see the ESI† for full computational details). Minimum-energy optimized geometries calculated at the B3LYP/cc-pVDZ level in CH_2Cl_2 indicated that the rhodanine moiety remained coplanar with the fluorene core in all four dyes, constituting both moieties on the central acceptor unit of the D–A–D architecture (see Fig. S7 in the ESI†). For **RFTA-3** and **RTFA-4**, the thiophene rings bridging the donor DPAT groups to the acceptor moiety were calculated to be almost coplanar with the fluorene core, with the largest dihedral angles of 8.9°. In contrast, the phenyl rings bridging the TPA units in **RFTA-1** and **RFTA-2** were 30–32° out of the plane of the fluorene core due to the steric hindrance caused by short H···H contacts (Fig. S7, in the ESI†). Finally, both TPA and DPAT units were calculated to show the typical mill sails shape.

The highest-occupied molecular orbitals (HOMO and HOMO−1) were predicted to be nearly degenerate and are localized on the two electron-donor fragments, either TPA or DPAT (see Fig. 2a for **RFTA-3**, as a representative example, and Fig. S8,† in the ESI,† for the rest of compounds). The higher conjugation and more planar structure promoted by the less-aromatic thiophene rings in **RFTA-3** and **RFTA-4** determined that the HOMOs of these dyes were computed to be higher in energy (−5.02 and −5.04 eV, respectively) than the HOMOs of **RFTA-1** and **RFTA-2** (−5.11 and −5.13 eV, respectively). Moreover, this provokes a certain splitting (0.07 eV) between the HOMO and HOMO−1. The increase of ∼0.1 eV in the HOMO energy confirms DPAT groups as better donors than TPAs and is in good agreement with the lower oxidation potentials obtained for **RFTA-3** and **RFTA-4** (Table 2). The lowest-unoccupied molecular orbital (LUMO) was located on the acceptor rhodanine–fluorene moiety for all four compounds. The LUMO was calculated at −3.07 eV for **RFTA-1** and **RFTA-3**, and it was computed to be ∼0.1 eV lower in energy for **RFTA-2** and **RFTA-4** due to the presence of the stronger electron-

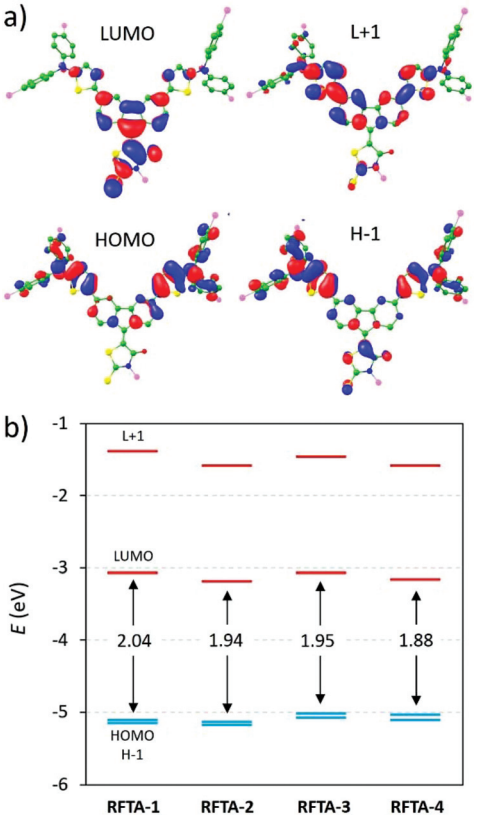

Fig. 2 (a) Isovalue contours (±0.025) calculated for the frontier MOs of **RFTA-3**. Alkyl chains and hydrogen atoms are omitted for better viewing. (b) Frontier MO energies, including the HOMO–LUMO gap, for the four rhodanine-based D–A–D dyes. H and L denote HOMO and LUMO, respectively.

accepting 2-(1,1-dicyanomethylene)rhodanine moiety. This result supports the less negative reduction potentials obtained for **RFTA-2** and **RFTA-4**.

Time-dependent density functional theory (TD-DFT) calculations were conducted to fully rationalize the nature and trends experimentally obtained for the low-lying absorption bands of the dyes. The 30 lowest-lying singlet excited states (S_n) were computed at the B3LYP/cc-pVDZ level in CH_2Cl_2 solution, and the main characteristic features of the most relevant excitations are shown in Table 3 for **RFTA-3** as a representative example (see Table S1 in the ESI† for all the dyes).

The lowest-lying broad absorption band observed in the UV-vis spectra of **RFTA-1–4** (Fig. 1) originated from the $S_0 \rightarrow S_1$ and $S_0 \rightarrow S_2$ transitions, which were described by the HOMO → LUMO and HOMO−1 → LUMO one-electron excitations, respectively. These excitations imply an electron transfer from the donor units, where the HOMO and HOMO−1 are located, to the electron-acceptor rhodanine–fluorene moiety, where the LUMO resides (see Fig. 2a). This confirmed the charge transfer character of the absorption band. The electronic transition to the S_1 state was calculated at 1.72 eV for **RFTA-1** and experienced a red-shift while moving to **RFTA-2** (1.63 eV) and **RFTA-3** (1.62 eV). The shift was attributed to the insertion of a stronger

Table 3 Singlet excited states calculated for **RFTA-3** at the TD-B3LYP/cc-pVDZ level in CH_2Cl_2

State	E^a (eV)	E^a (nm)	f^b	Description[c]	Nature[d]
S_1	1.62	767	0.560	H → L	D → A
S_2	1.80	687	0.658	H−1 → L	D → A
S_5	2.75	451	0.653	H−2 → L	A → A
S_6	3.08	403	0.503	H−5 → L	F → A
S_7	3.14	395	0.446	H−1 → L+1	D → A

[a] Vertical excitation energies (in eV and nm). [b] Oscillator strengths. [c] Description in terms of monoexcitations; H and L denote HOMO and LUMO, respectively. [d] Nature of the excited state; the labels A, D, and F refer to acceptor, donor, and fluorene-core moieties, respectively.

electron-acceptor group (7) for **RFTA-2** and to the enhanced electron-donor character of the DPAT moieties in **RFTA-3**. The inclusion of both acceptor/donor groups in **RFTA-4** led to an additional red-shift of the transition to the S_1 state computed at 1.56 eV, in good agreement with the experimental data. S_2 was predicted to follow similar trends (Table S1†). Interestingly, D–A–D dyes containing the DPAT unit (**RFTA-3** and **RFTA-4**) showed a larger separation between S_1 and S_2 (0.19 eV) compared to the dyes bearing TPA as a donor moiety (0.12 eV in **RFTA-1** and **RFTA-2**). This was ascribed to the more planar and better conjugated structures promoted by the thiophene rings of the DPAT units, and explains the broadening observed for the lowest-lying CT band while passing from **RFTA-1–2** to **RFTA-3–4** (Fig. 1). Moving to higher energies, the excited state associated with the HOMO−2 → LUMO excitation (S_5 for **RFTA-1** and **RFTA-3** and S_4 for **RFTA-2** and **RFTA-4**) was predicted to influence the shape of the band observed around 450 nm (Fig. 1). This state originated from a one-electron promotion centered on the rhodanine–fluorene acceptor moiety and was calculated at similar wavelengths (445–461 nm, Table S1†) for all four dyes. Finally, a large number of electronic excitations with a high multiconfigurational character were predicted in the 300–400 nm range. Specifically, the sharp bands experimentally obtained at 325 nm for **RFTA-1** and **RFTA-2** and the less-intense bands around 375 nm obtained for **RFTA-3** and **RFTA-4** (Fig. 1) originated from electronic excitations mainly centered on the donor and fluorene moieties.

Conclusions

In summary, a new family of dyes bearing rhodanine derivatives rigidly linked to a planar fluorene central core were synthesized and characterised for the first time. The new dyes show a very broad absorption band that covers all the visible region of the spectrum from 400 to 790 nm. Calculations demonstrated that this absorption implies the electronic transition to the S_1 (HOMO → LUMO) and S_2 (HOMO−1 → LUMO) excited states, which have a charge-transfer nature. The relatively high intensity exhibited by these transitions was due to the effective conjugation between the donor and acceptor

units through the fluorene core. Emission measurements showed that these dyes had large Stokes' shifts and were poor emitters, due to the strong CT character of the lower energy transition. From our observations, it may be concluded that dyes bearing the dicyanovinylene rhodanine acceptor fragment allowed a much broader absorption of the visible range of light, with electrochemical energy gaps between 1.4 and 1.5 eV, as previously reported.[22] Furthermore, it was demonstrated that a thienodiphenylamine donor fragment provided a more effective coupling with the acceptor due to the reduced dihedral angle allowed by the thiophene ring. The newly synthesized D–A–D dyes possess the necessary properties for their use in small molecule organic photovoltaics.

Acknowledgements

This work was funded by the European Commission (ERC-320441-Chirallcarbon), MINECO of Spain (CTQ2014-52045-R, CTQ2015-71154-P, Unidad de Excelencia María de Maeztu MDM-2015-0538), Comunidad de Madrid (FOTOCARBON-CM S2013/MIT-2841), Generalitat Valenciana (PROMETEO/2016/135), and European FEDER funds (CTQ2015-71154-P). J. C. thanks the MECD of Spain for a predoctoral FPU grant. NM thanks EC FP7 ITN "MOLESCO" Project no. 606728.

Notes and references

1 Progression can be followed from the National Renewable Energy Laboratory (NREL) webpage http://www.nrel.gov/ncpv/images.
2 S. E. Shaheen, C. J. Brabec, N. S. Sariciftci, F. Padinger, T. Fromherz and J. C. Hummelen, *Appl. Phys. Lett.*, 2001, **78**, 841–843.
3 C. J. Brabec, S. E. Shaheen, C. Winder, N. S. Sariciftci and P. Denk, *Appl. Phys. Lett.*, 2002, **80**, 1288–1290.
4 I. Riedel, E. von Hauff, J. Parisi, N. Martín, F. Giacalone and V. Dyakonov, *Adv. Funct. Mater.*, 2005, **15**, 1979–1987.
5 Y. Kim, S. Cook, S. M. Tuladhar, S. A. Choulis, J. Nelson, J. R. Durrant, D. C. Bradley, M. Giles, I. McCulloch, C.-S. Ha and M. Ree, *Nat. Mater.*, 2006, **5**, 197–203.
6 G. Dennler, M. C. Scharber and C. J. Brabec, *Adv. Mater.*, 2009, **21**, 1323–1338.
7 A. Sánchez-Díaz, M. Izquierdo, S. Filippone and N. Martín, *Adv. Funct. Mater.*, 2010, **20**, 2695–2700.
8 Y. Liu, J. Zhao, Z. Li, C. Mu, W. Ma, H. Hu, K. Jiang, H. Lin, H. Ade and H. Yan, *Nat. Commun.*, 2014, **5**, 5293.
9 Z. He, B. Xiao, F. Liu, H. Wu, Y. Yang, S. Xiao, C. Wang, T. P. Russell and Y. Cao, *Nat. Photonics*, 2015, **9**, 174–179.
10 L. J. Zuo, C. Y. Chang, C. C. Chueh, S. H. Zhang, H. Y. Li, A. K. Y. Jen and H. Z. Chen, *Energy Environ. Sci.*, 2015, **8**, 1712–1718.
11 J. Huang, J. H. Carpenter, C.-Z. Li, J.-S. Yu, H. Ade and A. K. Y. Jen, *Adv. Mater.*, 2016, **28**, 967–974.
12 W. Zhao, D. Qian, S. Zhang, S. Li, O. Inganäs, F. Gao and J. Hou, *Adv. Mater.*, 2016, **28**, 4734–4739.
13 B. Kan, M. Li, Q. Zhang, F. Liu, X. Wan, Y. Wang, W. Ni, G. Long, X. Yang, H. Feng, Y. Zuo, M. Zhang, F. Huang, Y. Cao, T. P. Russell and Y. Chen, *J. Am. Chem. Soc.*, 2015, **137**, 3886–3893.
14 J.-L. Wang, Q.-R. Yin, J.-S. Miao, Z. Wu, Z.-F. Chang, Y. Cao, R.-B. Zhang, J.-Y. Wang, H.-B. Wu and Y. Cao, *Adv. Funct. Mater.*, 2015, **25**, 3514–3523.
15 J. Min, C. Cui, T. Heumueller, S. Fladischer, X. Cheng, E. Spiecker, Y. Li and C. J. Brabec, *Adv. Energy Mater.*, 2016, 1600515.
16 J. Zhou, Y. Zuo, X. Wan, G. Long, Q. Zhang, W. Ni, Y. Liu, Z. Li, G. He, C. Li, B. Kan, M. Li and Y. Chen, *J. Am. Chem. Soc.*, 2013, **135**, 8484–8487.
17 C. A. Echeverry, A. Insuasty, M. A. Herranz, A. Ortíz, R. Cotta, V. Dhas, L. Echegoyen, B. Insuasty and N. Martín, *Dyes Pigm.*, 2014, **107**, 9–14.
18 S. Badgujar, G.-Y. Lee, T. Park, C. E. Song, S. Park, S. Oh, W. S. Shin, S.-J. Moon, J.-C. Lee and S. K. Lee, *Adv. Energy Mater.*, 2016, 1600228.
19 Y. Song, W. Xu and D. Zhu, *Tetrahedron Lett.*, 2010, **51**, 4894–4897.
20 V. Maurel, L. Skorka, N. Onofrio, E. Szewczyk, D. Djurado, L. Dubois, J.-M. Mouesca and I. Kulszewicz-Bajer, *J. Phys. Chem. B*, 2014, **118**, 7657–7667.
21 (*a*) T. Yatsuhashi, Y. Nakajima, T. Shimada and H. Inoue, *J. Phys. Chem. A*, 1998, **102**, 3018–3024; (*b*) L. Biczók, T. Bérces, T. Yatsuhashi, H. Tachibana and H. Inoue, *Phys. Chem. Chem. Phys.*, 2001, **3**, 980–985; (*c*) L. A. Estrada, J. E. Yarnell and D. C. Neckers, *J. Phys. Chem. A*, 2011, **115**, 6366–6375; (*d*) I. Ghosh, A. Mukhopadhyay, A. L. Koner, S. Samanta, W. M. Nau and J. N. Moorthy, *Phys. Chem. Chem. Phys.*, 2014, **16**, 16436–16445.
22 Q. Zhang, B. Kan, F. Liu, G. Long, X. Wan, X. Chen, Y. Zuo, W. Ni, H. Zhang, M. Li, Z. Hu, F. Huang, Y. Cao, Z. Liang, M. Zhang, T. P. Russell and Y. Chen, *Nat. Photonics*, 2015, **9**, 35–41.